NASTRAN BUCKLING STUDY OF A LINEAR INDUCTION MOTOR REACTION RAIL

By Jerry G. Williams

NASA Langley Research Center
Hampton, Virginia

ABSTRACT

NASTRAN was used to study problems associated with the installation of a linear induction motor reaction rail test track at the Department of Transportation High-Speed Ground Test Center near Pueblo, Colorado. Specific problems studied include determination of the critical axial compressive buckling stress and establishment of the lateral stiffness of the reaction rail under combined loads. NASTRAN results were compared with experimentally obtained values and satisfactory agreement was obtained. The reaction rail was found to buckle at an axial compressive stress of 78.6 MN/m^2 (11 400 lb/in^2). The results of this investigation were used to select procedures for installation of the reaction rail at the Pueblo test site.

INTRODUCTION

Linear induction motor propulsion systems for high-speed ground transportation vehicles are being tested by the U.S. Department of Transportation at its High-Speed Ground Test Center near Pueblo, Colorado. One of these vehicles, the Linear Induction Motor Research Vehicle (LIMRV) (see fig. 1), has a linear induction motor approximately 3 m (10 feet) long which exerts axial force against a vertical aluminum reaction rail supported by conventional crossties of a railroad track (ref. 1). The reaction rail is a thin plate-like member which is fusion welded into a continuous strip before clamping it to the crossties. It experiences thermal loads because of ambient temperature variations and localized axial loads which react the thrust of the linear induction motor. The axial loads are small in comparison to the thermal loads and are not considered in this study. In addition, lateral loads are imposed on the reaction rail by the guide wheels of the linear induction motor. A drawing showing the rail cross section and its attachment hardware is presented in figure 2.

The expected reaction rail temperature extremes at the test center range from 239 K (-30° F) to 333 K (140° F). Since there are no expansion joints in the reaction rail, normal atmospheric temperature variations cause the rail stresses to change as a function of the ambient temperature. For example, if the rail is installed at 333 K, compressive stresses will not be developed but the tensile stresses will be high at low temperatures. A stress-free installation temperature T_o between 239 K and 333 K subjects the rail to compressive stress when the rail temperature exceeds T_o and tensile stress when the temperature is lower than T_o.

Potential problems associated with compressive loading of the reaction rail, including buckling and reduced lateral stiffness, have been studied by using NASTRAN and by laboratory experiments. A detailed description of experimental procedures and results is presented in reference 2. A special-purpose finite-difference solution to the classical plate equations with appropriate boundary conditions was also formulated and these results are presented and compared with selected NASTRAN results in reference 3. The current paper presents additional results, provides details of the NASTRAN model, and makes comparisons between NASTRAN and experimental results for the critical buckling stress and the lateral displacement response of the rail under combined axial and compressive loads. Suggestions are also proposed for an improved reaction rail geometry.

NASTRAN MODEL

A drawing of the NASTRAN model used to represent the reaction rail is presented in figure 3. A rail length of 5.56 m (219 inch) was selected for study based on preliminary NASTRAN calculations which showed the critical buckling stress for this length rail to be nearly independent of the boundary conditions imposed on the rail ends. This insensitivity to end boundary conditions is important since it implies that it is unnecessary to define the exact boundary conditions imposed on the ends of a typical section selected from the continuous long-length test track. Geometric symmetry about the specimen midlength permitted the problem to be represented analytically by a model which included only half of the specimen length. A rectangular network of isotropic bending plus membrane quadrilateral plate elements (CQUAD2) was used to represent both the vertical web and base flange components.

At any given axial station, the rail vertical web was represented by seven plate elements and the base flange by four plate elements. Axially, the half-rail was represented by 34 plate elements. The center two base flange elements had cross-sectional dimensions of 4.53 cm (1.785 in.) wide and 1.0 cm (0.40 in.) thick while the two outer-base flange elements had cross-sectional dimensions of 1.82 cm (0.715 in.) wide and 0.79 cm (0.312 in.) thick. The vertical web voids were accounted for in the analysis by giving the isotropic quadrilateral plate elements an equivalent bending stiffness of 20.6 kN m (182 600 in-lb) which was calculated by treating the web as a sandwich plate and neglecting the separators between voids. This stiffness representation was verified by comparing NASTRAN and experimental results for the lateral displacement response of a 2.54 cm (1 in.) long section of rail loaded by a 445-N (100-lb) lateral force located at a height of 34.3 cm (13.5 in.) measured from the rail base flange. NASTRAN results compared favorably with experimental measurements as can be seen in figure 4.

Clamped boundary conditions were imposed at the rail end while both symmetry and antisymmetry conditions were considered at the rail midlength to insure that the lowest buckling solution was obtained. The restraint to displacement imposed by clamps mounted to wooden crossties every 0.483 m (19 in.) along the rail base flange was modeled analytically by a set of

30

horizontal and vertical springs discretely located along the free edge of base flange elements. Mathematical ill-conditioning was experienced under certain conditions when the spring constants were specified by a CEL S1 data card. This problem was overcome by representing the spring constants by CROD data cards in which a unit area rod had the required axial stiffness and zero torsional stiffness. The horizontal and vertical spring constant magnitudes were determined experimentally for the laboratory setup to be 12.6 and 75.3 MN/m per clamp (72 000 and 430 000 lb/in. per clamp), respectively. Details of the technique used to measure these properties are reported in reference 2. For comparison, calculations were also made assuming the clamps to be fully restrained.

Axial stress was thermally introduced into the NASTRAN model as a result of restraining the rail ends against axial displacement and introducing a near isothermal temperature increase. Lateral loading was introduced by applying a concentrated load at the model midlength and 15.2 cm (6 in.) below the top edge of the rail. Calculations were made with NASTRAN level 15 version. Buckling solutions were obtained by use of the inverse power method of eigenvalue extraction (rigid format 5) and lateral stiffness calculations were made by use of the differential stiffness capability (rigid format 4).

As a check on modeling and problem formulation, the axially loaded classical plate-buckling problem in which the two vertical ends and the lower edge are clamped and the upper edge is free was solved using NASTRAN. The plate size and model characteristics, except for the difference in lower edge boundary and absence of the base flange, were identical to those for the rail problem. The NASTRAN finite-element solution showed almost exact agreement with the known solution (ref. 4). This agreement gave confidence that the model was well formulated and that grid-point spacing was sufficiently refined.

Typical Langley Research Center costs to compute the critical buckling stress for the reaction rail model which had approximately 2000 degrees of freedom using a CDC 6600 computer was $325. This cost included approximately 1700 CPU seconds and 28000 O/S calls and was run at a field length of 155 000$_8$. Lateral stiffness calculations cost approximately $220 and included approximately 1250 CPU seconds and 18000 O/S calls.

EXPERIMENT

The laboratory test setup involved clamping a 5.56-m (219-in.) length of reaction rail to the center line of wooden crossties spaced every 0.483 m (19 in.) in a fashion representative of the field installation method. This length included a 13-cm (5-in.) section at each end of the rail between the last base flange clamp and the end fixture. Clamped boundary conditions were imposed at the rail ends. Rail crossties and clamp hardware were taken from stock used in the Pueblo field installation. Axial compressive stress in the rail was developed by restraining the ends against axial displacement and heating the rail in a near isothermal manner using radiant heater panels.

31

Thermocouples were used to measure the rail temperature, strain gages were used to determine stresses, and linear voltage differential transducers (LVDT) were used to measure lateral displacements. The electronic output was recorded automatically and stored on magnetic tape for later reduction. A detailed description of the test technique is reported in reference 2 and a photograph of the laboratory setup is presented in figure 5.

Buckling and lateral stiffness experiments were conducted on each of two reaction rail specimens. Prior to each test, the rail was surveyed and, when necessary, shims were used to obtain the desired conditions of straightness. A brief description of these two experiments is presented below.

Buckling of a "Well-Alined" Rail

In this test the specimen was heated to induce axial compressive stress until large lateral deformations were observed. The term "well-alined" indicates a specimen which was installed as nearly straight on the test bed as was practical. Typically, the upper edge and base flange were laterally alined within ±0.38 mm (±0.015 in.) and ±0.13 mm (±0.005 in.), respectively, of a straight line drawn through the end points of the rail. This arrangement is considerably better than that normally achieved in the field. The purpose of this experiment was to define the rail buckling stress and mode shape and to determine whether large lateral deformations are elastic.

Lateral Stiffness Test

This test involved applying a lateral point load at the rail midlength and 15.2 cm (6 in.) below the top edge in combination with selected magnitudes of axial stress. The purpose of this experiment was to determine the lateral stiffness of the rail as a function of the applied axial compressive stress. Lateral stiffness as used in this report is defined as the ratio of the lateral point load to the lateral displacement at the point of application of the load.

RESULTS

Buckling

Theoretical and experimental buckling results for a "well-alined" rail are presented in table I. Two NASTRAN solutions are presented, one in which the base flange clamps were spring supported and the other in which the base flange clamps were fully restrained (displacements and rotations set equal to zero). The critical buckling stress for the case in which the flange clamps were spring supported is 86.2 MN/m^2 (12 500 lb/in^2) which is approximately 7 percent lower than the solution in which the base flange clamps were fully restrained. In both cases the lowest buckling stress was obtained with symmetry boundary conditions imposed at the specimen midlength.

32

The experimentally obtained critical buckling stress was 78.6 MN/m^2 (11 400 lb/in^2) which is 9 percent lower than the NASTRAN spring-supported clamp solution. The experimental value corresponds to a rail temperature rise of 49.1 K (88.4° F) from a stress-free state.

The classical buckling solution of a rectangular plate with properties identical to the rail vertical web which is clamped on the ends and free on the top edge is 37.0 MN/m^2 (5400 lb/in^2) for the lower edge continuously simply supported and 111.4 MN/m^2 (16 200 lb/in^2) for the lower edge continuously clamped (ref. 2). These two extremes in boundary conditions bracket the base flange support conditions and the reaction-rail base flange/clamp-support system results fall approximately midway between the results for the continuous simple support and clamped conditions.

A comparison of NASTRAN and experimental results for the buckling lateral displacement of a line 2.54 cm (1 in.) below the rail upper edge is presented in figure 6. The axial distance from the center line is normalized by the rail height (0.533 m (21 in.)) and lateral displacements are normalized by the maximum displacement magnitude (which occurs at the top edge and center of the rail). The experimental mode shape is not symmetric about the center line, but is biased to the right. This irregularity may have been caused by variations in base flange support conditions. Both NASTRAN and experimental results exhibit a buckling mode shape of five half-waves for the 5.56 m (219-in.) long specimen. The midspan half-wave length given by both NASTRAN and the experiment was approximately 1 m (39.4 in.). A photograph of the buckled rail is presented in figure 7.

Lateral Stiffness

The normal operating clearance between the linear induction motor and the reaction rail is only 2.22 cm (0.875 in.) which sets an upper limit on the permissible peak-to-peak amplitude of lateral displacements. The lateral stiffness of the reaction rail is important not only to static load consideration but also to the dynamic performance of the LIMRV. Although this study addresses only the static behavior of the reaction rail, rail properties necessary for conducting a dynamic analysis were obtained. As indicated earlier, lateral stiffness is defined as the ratio of the lateral point load to the lateral deflection produced at the point of application of the load. The point lateral load in this study was located at the center of the specimen and 15.2 cm (6 in.) below the rail upper edge. The vertical location was selected to coincide with a position half-way between the upper and lower guidance wheels at one end of the linear induction motor. Experimentally, loads of up to 7560 newtons (1700 lb) were applied and lateral displacements as great as 1.9 cm (0.75 in.) were experienced. In all cases the rail elastically reacted the loads and returned to its original configuration upon release of the load.

The variation in lateral spring constant with axial compressive stress is presented in figure 8. The experimental results show a lateral spring constant of 820 kN/m (4680 lb/in.) at zero stress which decreases nearly

linearly to a value of 350 kN/m (2000 lb/in.) at an axial compressive stress of 74.5 MN/m^2 (10 800 lb/in^2). The NASTRAN solution in which the base flange clamps were fully restrained is only slightly lower than the experimental result (e.g., by only 5 percent for zero axial stress). The effect of representing the clamps by horizontal and vertical springs is to reduce the lateral stiffness by approximately 6 percent over the fully restrained condition.

The lateral displacement of the vertical portion of the rail corresponding to 35.6 MN/m^2 (5160 lb/in^2) axial stress and a lateral load of 4448 N (1000 lb) obtained using NASTRAN is presented in the displacement contour plot of figure 9. Displacements have been normalized with respect to the maximum amplitude which has been scaled to a value of 100. The maximum amplitude is approximately 1.14 cm (0.45 in.) and occurs at the midlength and upper edge of the rail. In this NASTRAN solution, the clamps were modeled as horizontal and vertical springs.

In addition to reducing the rail lateral stiffness, axial compressive stress also affects the lateral displacement field of a laterally loaded rail. This effect is shown in figure 10 in which the lateral displacements of a line located 2.54 cm (1 in.) below the upper edge are plotted for three magnitudes of axial stress in combination with a lateral load of 4447 N (1000 lb). An increase in the applied axial stress causes an increase in the maximum displacement amplitude and a decrease in the midspan effective wave length. As the axial compressive stress approaches the buckling stress, the combined load results in a distorted five half-wave buckled mode shape biased in the direction of the applied lateral load. NASTRAN and experimental results are in good agreement for an axial stress of zero and 35.6 MN/m^2 (5160 lb/in^2). Experimental results are not available for an axial stress of 71.2 MN/m^2 (10 300 lb/in^2) since 4448 N (1000 lb) lateral load in combination with this axial load would have resulted in unacceptably large lateral displacements. Lower magnitudes of lateral load for this axial stress, however, did establish the distorted five half-wave pattern indicated by the NASTRAN solution.

Improved Rail Design

A parametric study was made to determine the increase in the critical buckling stress resulting from an increase in the bending stiffness of the lower portion of the rail vertical web. The portion considered was the lower one-seventh of the vertical web (7.62 cm (3 in.) measured from the vertical web/base flange intersection). Results of this study are presented in figure 11 where the reference bending stiffness and the reference critical buckling stress are those of the previously described model.

A 25-percent increase in the critical buckling stress is obtained by increasing the bending stiffness by a factor of 8. This increase can be accomplished for the subject rail by taking the same cross-sectional area and increasing the total thickness of the lower portion of the vertical web to a

dimension of approximately 5.5 cm (2.2 in.). This approach may have merit in the geometric design of future reaction rails which react to compressive loading subject, of course, to geometric constraints imposed by the linear induction motor.

CONCLUDING REMARKS

Satisfactory agreement was achieved between NASTRAN and experimental results for the buckling load, buckling mode shape, lateral displacement response to a point lateral load, and lateral stiffness of the reaction rail as a function of axial load. Parametric studies of the stiffness of the lower portion of the reaction rail indicate substantial improvements can be obtained in the critical buckling stress by increasing the lower portion bending stiffness.

The results of this investigation show that substantial axial compressive loads can be carried by the LIMRV reaction rail without buckling. Furthermore, lateral deformations up to 1.9 cm (0.75 in.) are elastic and disappear upon release of the imposed loads. The latter result means that even if the reaction rail is installed at a stress-free temperature which is later exceeded by sufficient magnitude to cause buckling, the event is not cata-strophic if test operations are suspended for this interim period.

Based on these results, the recommendation was given the Department of Transportation that the LIMRV reaction rail test track be installed at a stress-free temperature of around 297 K (75° F). The predicted buckling temperature, based on a 78.6-MN/m^2 (11 400-lb/in^2) buckling stress, would then be 346 K (163° F) which is higher than the rail can experience through solar heating at the test center. This recommendation was adopted by the Department of Transportation in the fall of 1972 in the installation of the Pueblo test track. Successful operation of the LIMRV has been in progress since that time with no problems encountered with the reaction rail.

REFERENCES

1. Anon.: Linear Induction Motor Research. Vol. I, Rep. 71-7094, AiResearch Manufacturing Co., Oct. 1971. (Available as NTIS PB 212-041.)

2. Haight, E. C.; Hutchens, W. A.; and Williams, J. G.: Experimental Determination of the Compressive Behavior of a Linear Induction Motor Reaction Rail. MTP-374, The Mitre Corp., Nov. 1, 1972. (Available as NTIS PB 214-506.)

3. Williams, Jerry G.; Haight, Edward C.; and Hutchens, Walter A.: Compressive Behavior of a Linear Induction Motor Rail. Paper to be presented at Intersociety Transportation Conference (Denver, Colorado), September 24-27, 1973.

4. Lundquist, Eugene E.; and Stowell, Elbridge Z.: Critical Compressive Stress for Outstanding Flanges. NACA Rep. 734, 1942.

TABLE I. COMPARISON OF THEORETICAL AND EXPERIMENTAL

BUCKLING RESULTS FOR A WELL-ALINED RAIL

	Buckling stress, MN/m^2 (lb/in²)	Temperature rise to buckle, K (°F)	Buckling half-wave length,[1] m (in.)
NASTRAN Base flange clamps spring supported[2]	86.2 (12 500)	53.8 (96.9)	1.03 (40.5)
NASTRAN Base flange clamps fully restrained	92.4 (13 400)	57.7 (103.9)	1.00 (39.4)
Experiment	78.6 (11 400)	49.1 (88.4)	0.97 (38.2)

[1]Half-wave length measured at center of specimen or model.
[2]Clamp horizontal and vertical spring constants equal 12.6 and 75.3 MN/m per clamp (72 000 and 430 000 lb/in. per clamp), respectively.
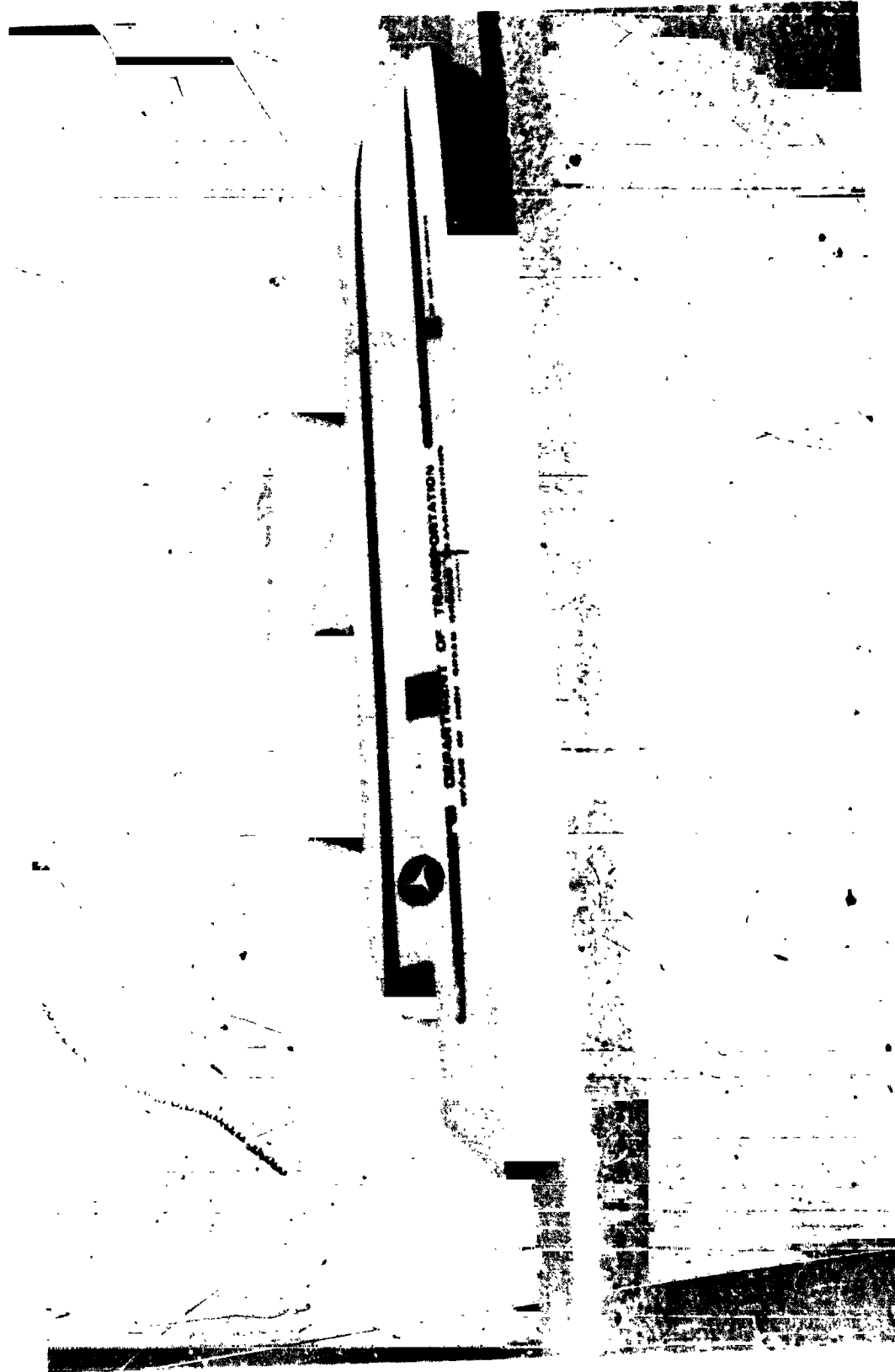
Figure 1. Linear Induction Motor Research Vehicle (LIMRV).

REACTION RAIL

SHIM, TIE PLATE

SCREW
SPRING CLIP

WOODEN TIE

TIE PLATE

.330 cm TYP

.330 cm

54.5 cm

1.59 cm

3.48 cm

6.35 cm

.792 cm

1.11 cm REF

12.700 cm
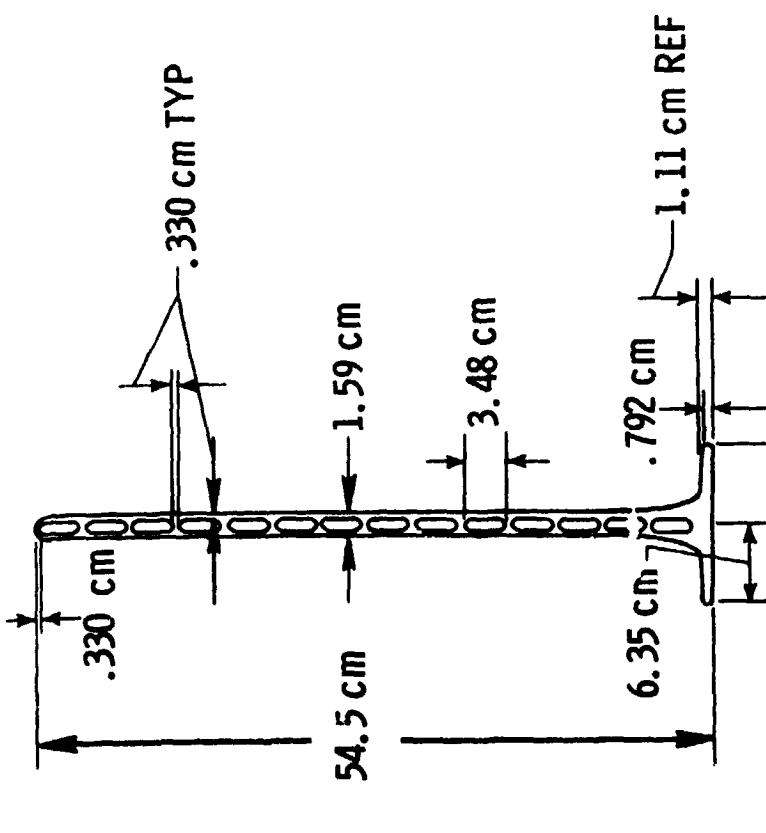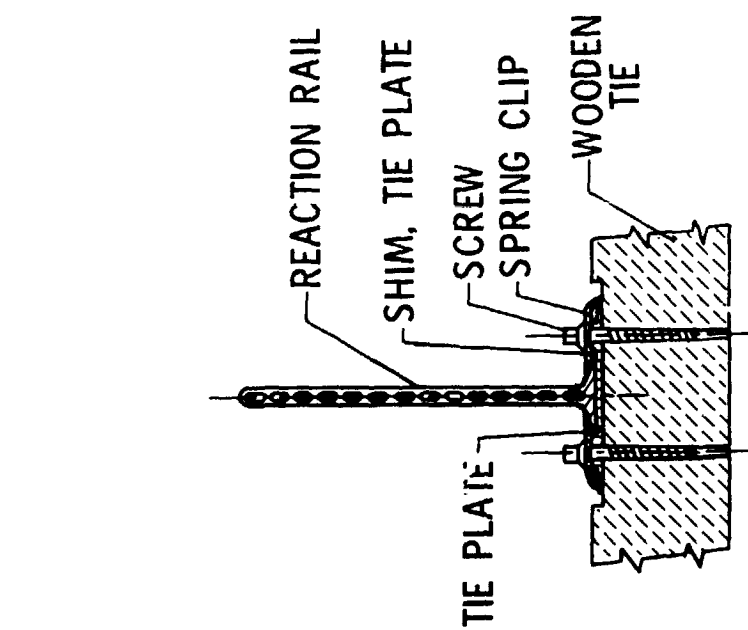
MODULUS OF ELASTICITY = 69.0 GN/m^2
POISSON'S RATIO = 0.3
CROSS-SECTIONAL AREA = 55.94 cm^2
COEFFICIENT OF LINEAR EXPANSION = 2.32 × 10^{-5} m/m/K
MASS PER UNIT LENGTH = 15.5 kg/m

Figure 2. Reaction rail dimensions and attachment hardware.
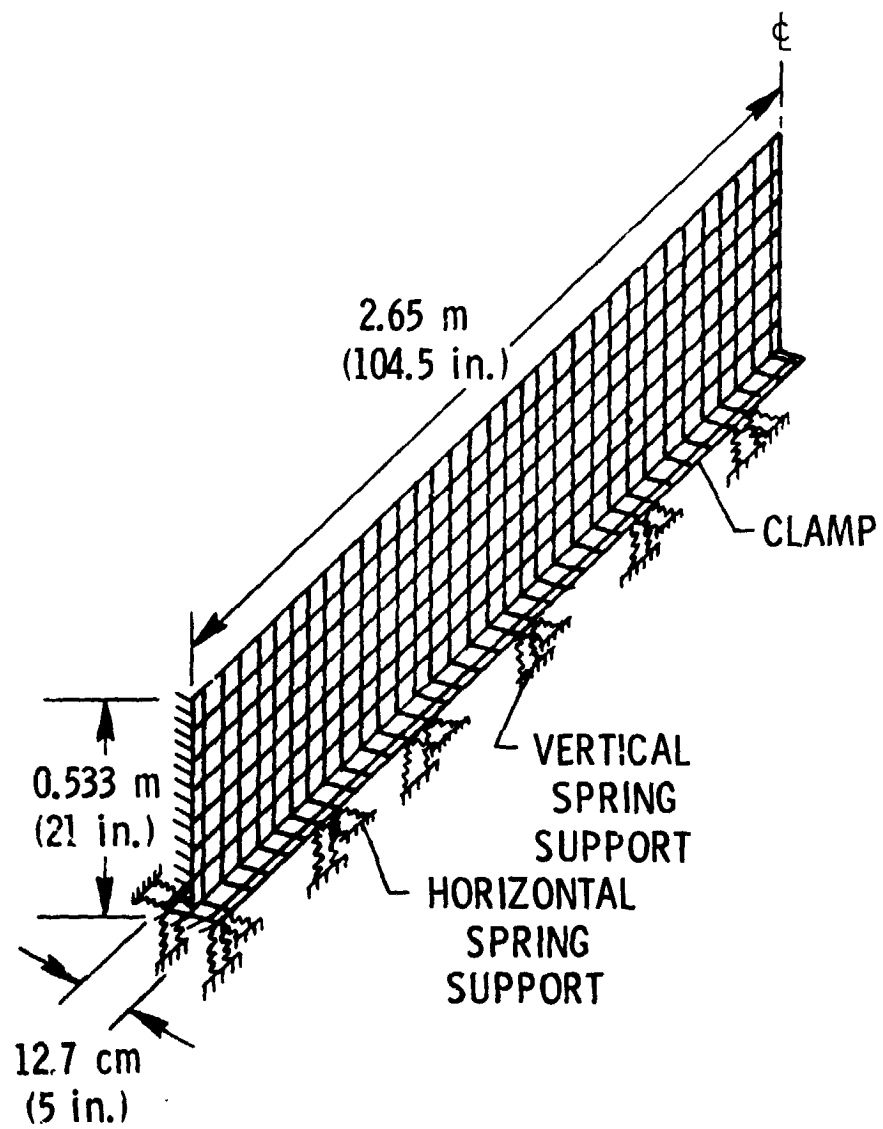
Figure 3.   NASTRAN model.
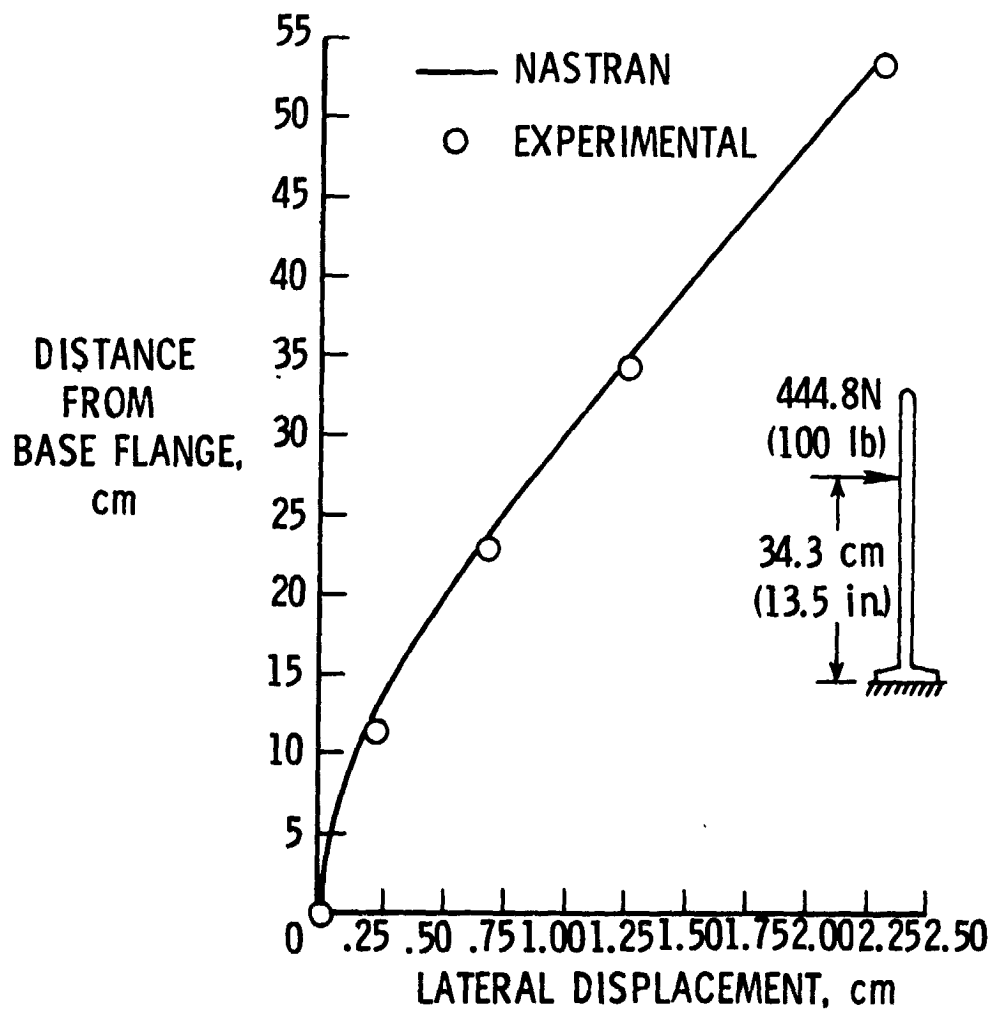
Figure 4. Lateral displacement of 2.54 cm (1 in.) long rail section due to 444.8N (100 lb) lateral load applied 34.3 cm (13.5 in.) above the base flange.

STRAIN GAGES
HEATER PANEL
LVDT INSTRUMENTATION
CLAMP
RAIL SPECIMEN
END FIXTURE
THERMOCOUPLE
CROSS TIE
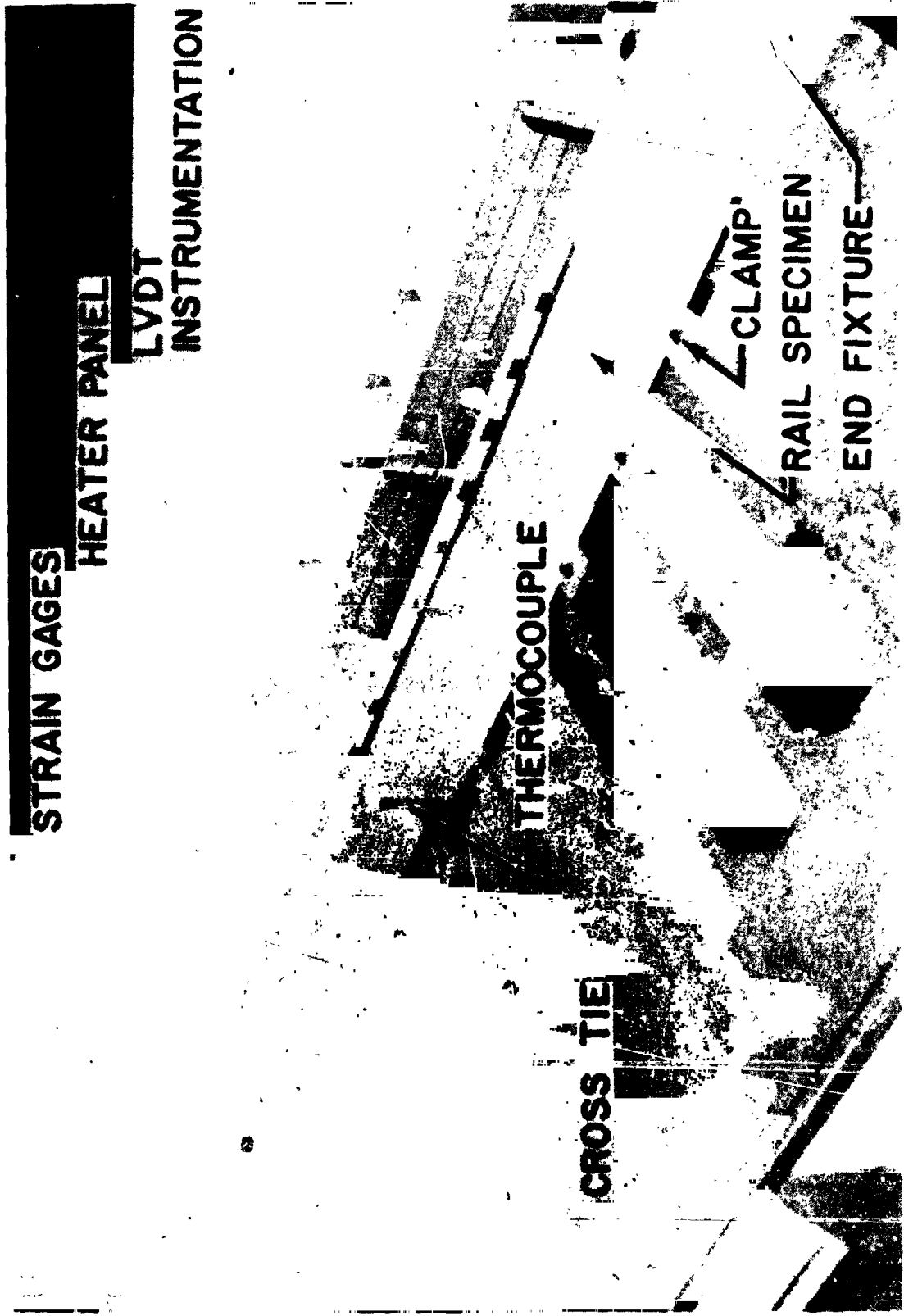
Figure 5. Experimental test setup.
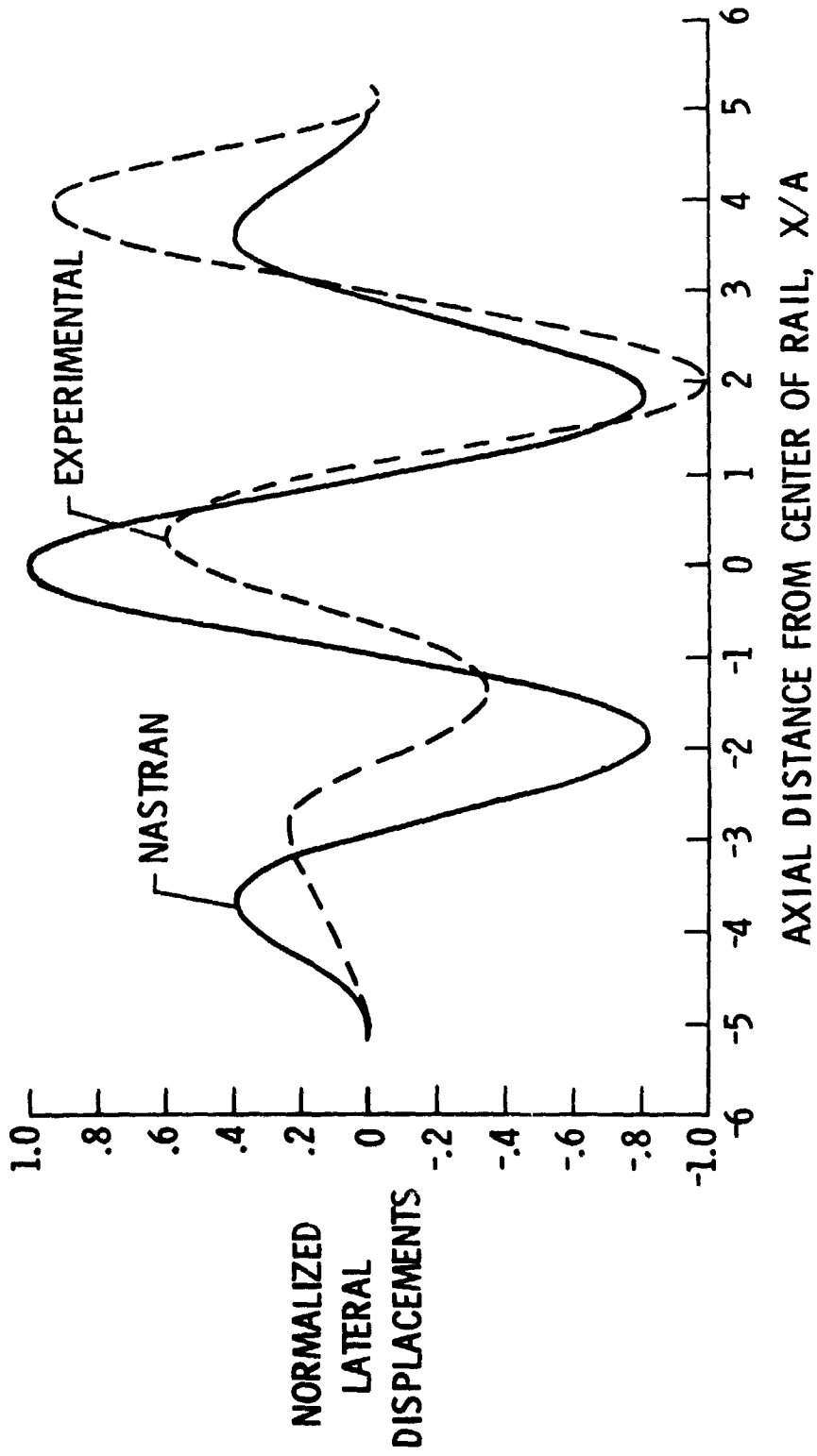
Figure 6. Buckled mode, theoretical and experimental deflections of line 2.54 cm (1 in.) from rail top edge. A is the rail height equal to 0.533 m (21 in.).
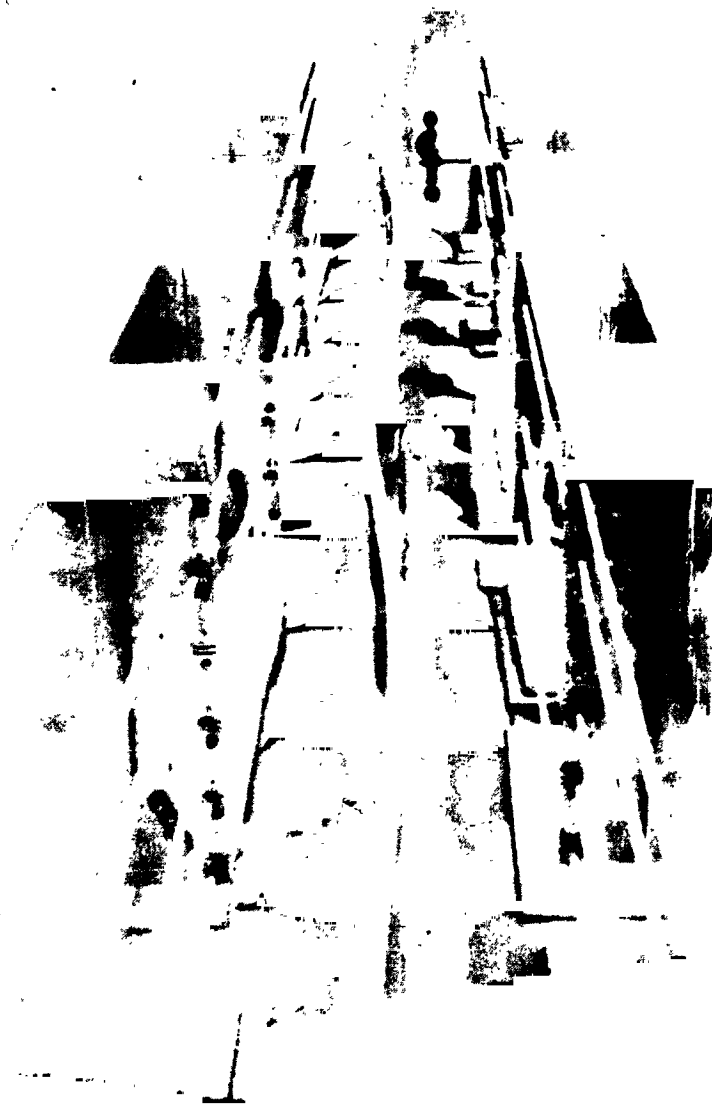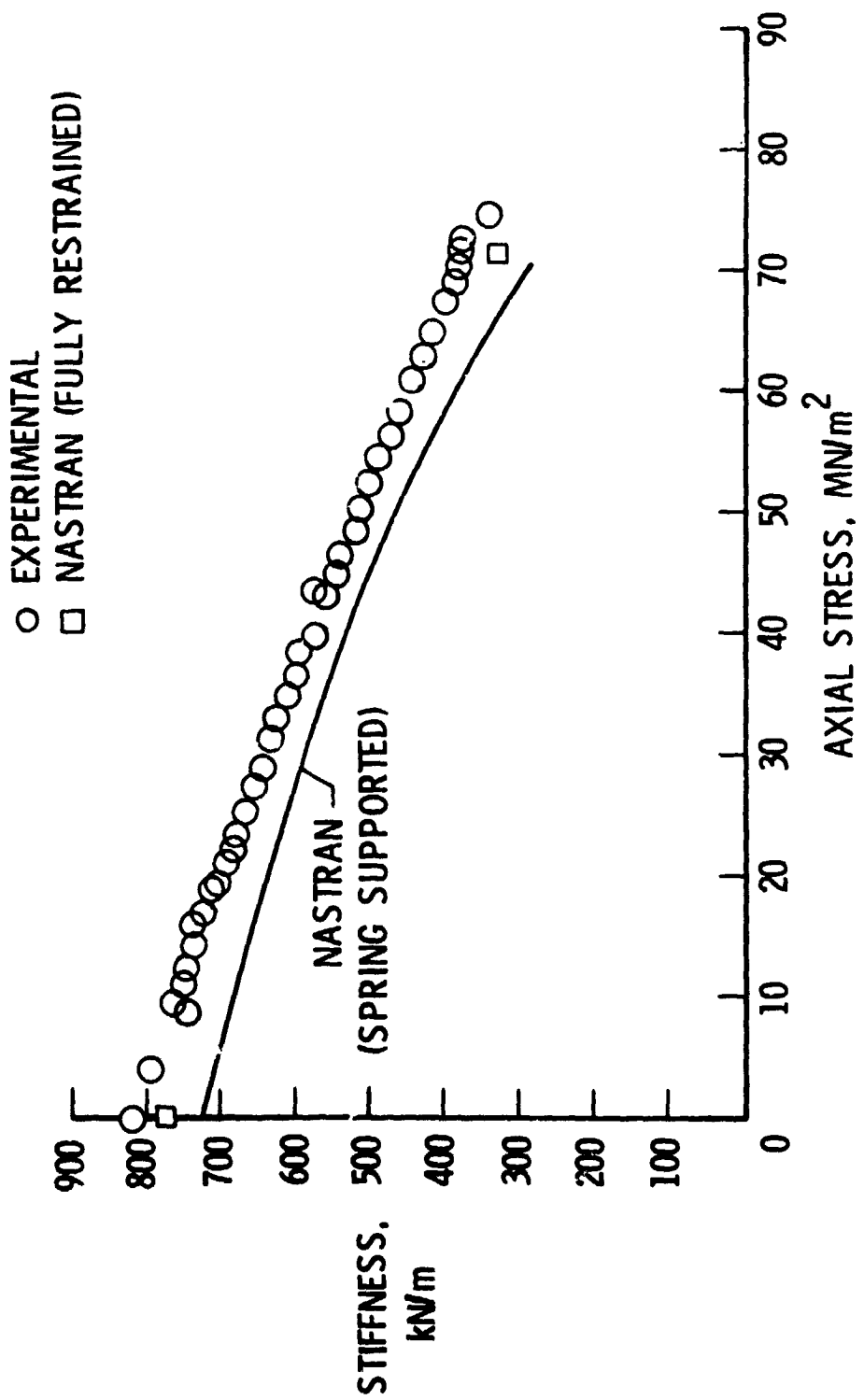
Figure 7. Buckled rail.

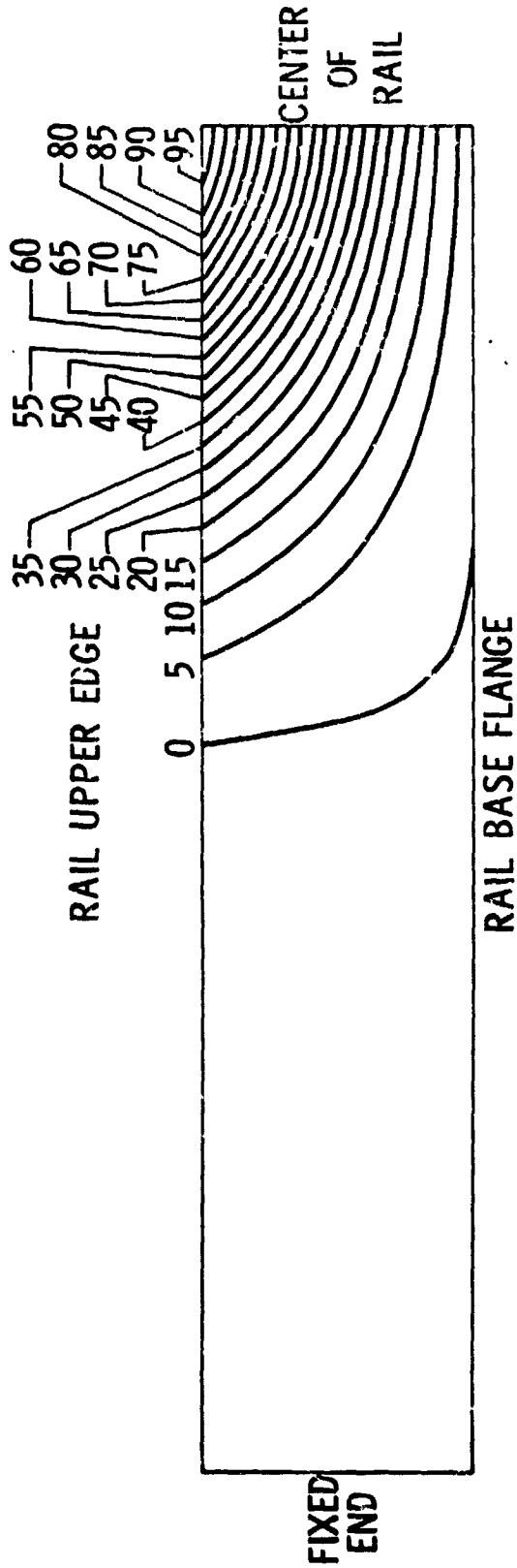Figure 8. Variation of rail lateral stiffness with axial stress.

Figure 9. Normalized contour plot for displacements of vertical web under combined axial stress (35.6 MN/m^2 (5160 lb/in.^{2})) and 4448 N (1000 lb) lateral load. Maximum amplitude equal 1.14 cm (0.45 in.).
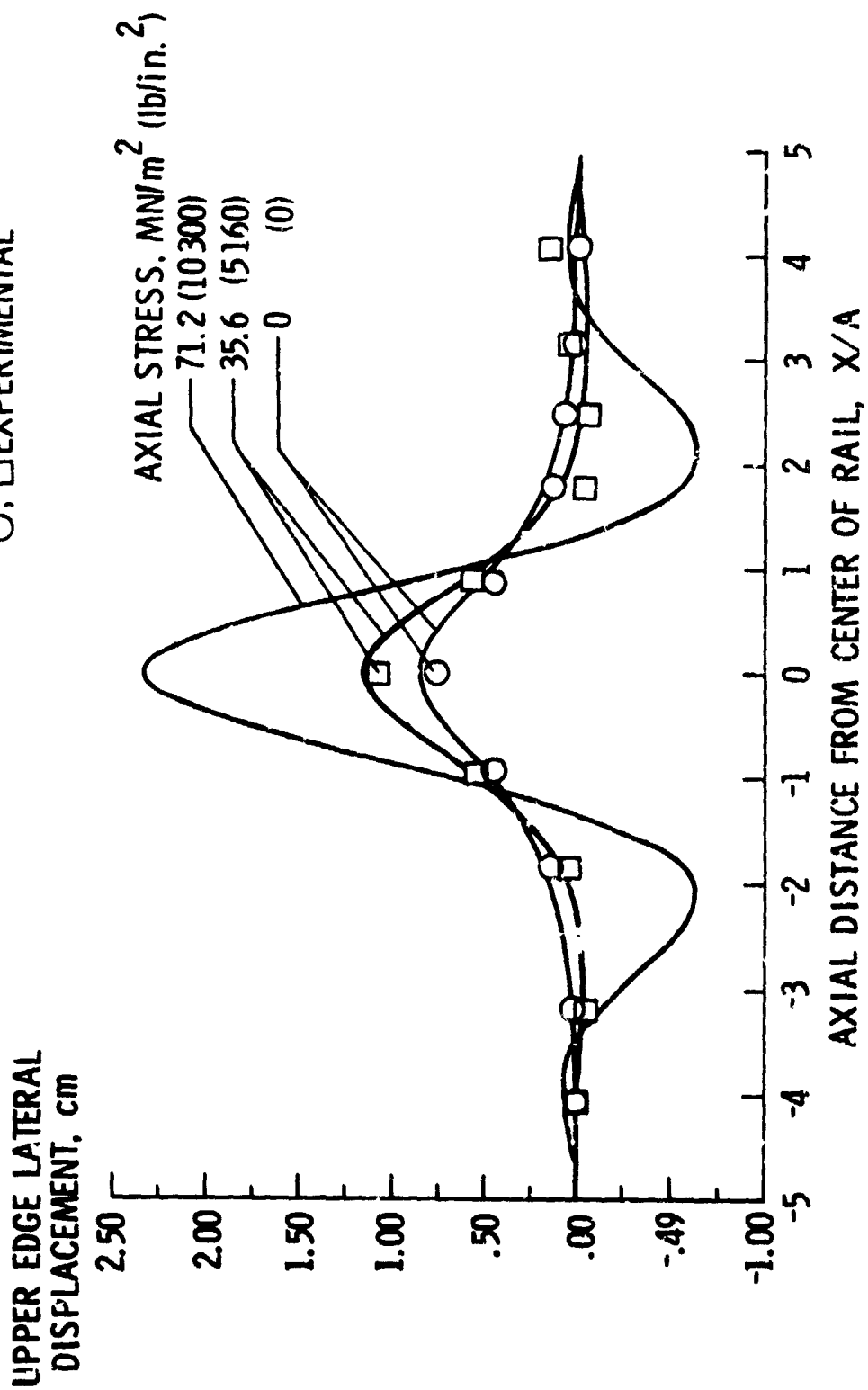
46

Figure 10. Lateral deflections of line 2.54 cm from rail top edge, 4448 N (1000 lb) lateral load and selected magnitudes of axial stress. A is the rail height equal to 0.533 m (21 in.).
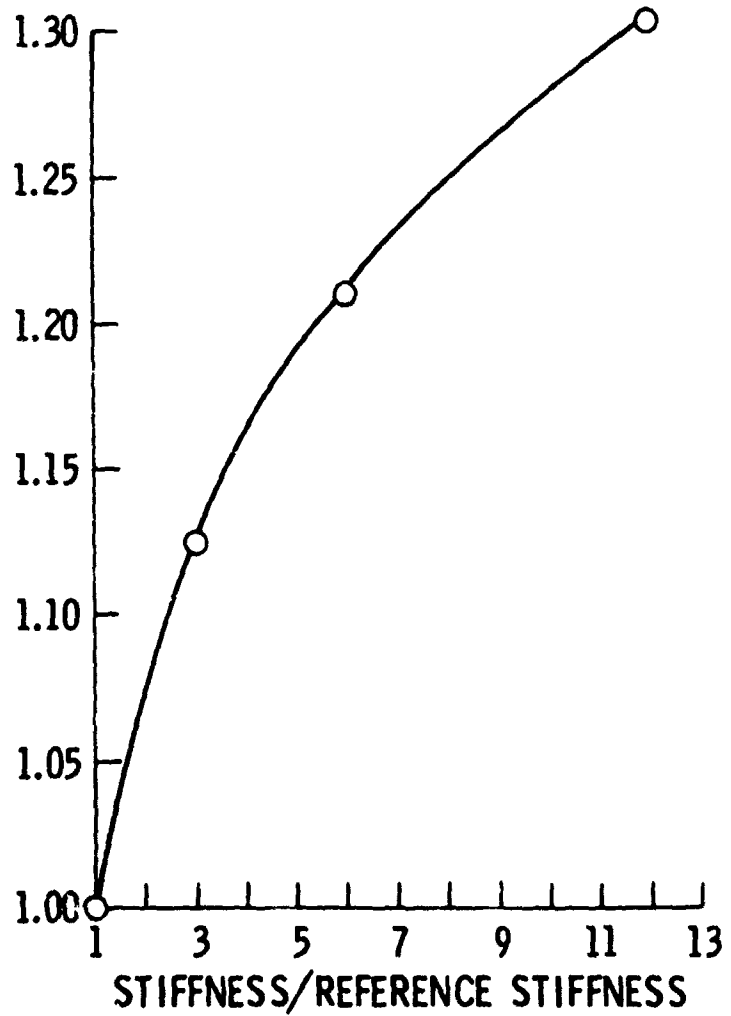
47

Figure 11. Variation of increase in critical buckling stress with increased bending stiffness of lower 7.62 cm (3 in.) of rail vertical web.